Environmental Pollution 205 (2015) 299–306

Contents lists available at ScienceDirect

Environmental Pollution

journal homepage: www.elsevier.com/locate/envpol

Fractionation in position-specific isotope composition during vaporization of environmental pollutants measured with isotope ratio monitoring by ^{13}C nuclear magnetic resonance spectrometry

Maxime Julien [a], Julien Parinet [b], Pierrick Nun [a], Kevin Bayle [a], Patrick Höhener [b], Richard J. Robins [a], Gérald S. Remaud [a, *]

[a] EBSI Team, CEISAM, University of Nantes-CNRS UMR 6230, 2 rue de la Houssinière BP 92208, F-44322 Nantes, France
[b] University of Aix-Marseille-CNRS, Laboratoire Chimie Environnement FRE 3416, Place Victor Hugo 3, 13331 Marseille, France

ARTICLE INFO

Article history:
Received 28 January 2015
Received in revised form
19 May 2015
Accepted 22 May 2015
Available online xxx

Keywords:
Position-specific isotope analysis
Isotope ratio monitoring by ^{13}C NMR spectrometry
Methyl *tert*-butylether
Trichloroethene
Vaporization

ABSTRACT

Isotopic fractionation of pollutants in terrestrial or aqueous environments is a well-recognized means by which to track different processes during remediation. As a complement to the common practice of measuring the change in isotope ratio for the whole molecule using isotope ratio monitoring by mass spectrometry (irm-MS), position-specific isotope analysis (PSIA) can provide further information that can be exploited to investigate source and remediation of soil and water pollutants. Position-specific fractionation originates from either degradative or partitioning processes. We show that isotope ratio monitoring by ^{13}C NMR (irm-^{13}C NMR) spectrometry can be effectively applied to methyl *tert*-butylether, toluene, ethanol and trichloroethene to obtain this position-specific data for partitioning. It is found that each compound exhibits characteristic position-specific isotope fractionation patterns, and that these are modulated by the type of evaporative process occurring. Such data should help refine models of how remediation is taking place, hence back-tracking to identify pollutant sources.

1. Introduction

Both the detection and quantification of pollutants and the cleaning-up of contaminated soil, sediment, or water are of great concern for the environmental industry. Among the analytical techniques available to identify the sources of pollutants, and/or to monitor their fate, isotope analysis has already proved efficient and widely applicable (Aelion et al., 2010). The bulk ^{13}C content, $\delta^{13}C_{bulk}$ (see Table S1 for the definitions of symbols used in the paper) can be measured by several techniques on the CO_2 produced by complete combustion of the sample. These include mass spectrometry (Muccio and Jackson, 2009), high resolution absorption measurements in the near-infrared (NIR) spectral range based on cavity ring-down spectroscopy (CRDS) (Crosson et al., 2002), and multi-collector inductively coupled plasma mass spectrometry (MC-ICPMS) (Malinovsky et al., 2013; Santamaria-Fernandez et al., 2008). The $^{13}C/^{12}C$ ratios of organic matter are most commonly determined by mass spectrometry, a technique correctly named irm-MS (isotope ratio monitoring by Mass Spectrometry) (Böttcher and Schnetger, 2004; Brand, 1996; Ellis and Fincannon, 1998; Smallwood et al., 2002). This technique (Galimov, 2006; Matthews and Hayes, 1978; Sano et al., 1976) can consistently measure the isotopic composition with a high precision, ~±0.1‰, when the configuration is OFF-line and ~±0.3‰ in the ON-line mode. Furthermore the method is very sensitive, making possible the study of dilute samples ((Muccio and Jackson, 2009) and references therein). When interfaced to a chromatography system, irm-MS is able to measure the δ_{bulk} of individual components within a matrix, leading to Compound-Specific Isotope Analysis (CSIA). CSIA is currently widely applied to the study of environmental problems (sources, processes, fate and (bio)remediation) using the main elements of organic matter ^{13}C, ^{2}H, ^{18}O, ^{15}N, ^{34}S (for recent reviews see (Elsner et al., 2012; Hofstetter and Berg, 2011; Thullner et al., 2012)) and also other elements such as ^{37}Cl and ^{81}Br (Cincinelli et al., 2012).

Nevertheless, this technique only determines the bulk isotope composition, thus ignoring any intramolecular variation in isotope pattern, the isotopologues. Furthermore, fractionation at one or two positions can be diluted out in the bulk measurement. An

* Corresponding author.
E-mail address: gerald.remaud@univ-nantes.fr (G.S. Remaud).

http://dx.doi.org/10.1016/j.envpol.2015.05.047
0269-7491/

approach has been proposed to compensate for this dilution effect inherent to the use of the bulk enrichment factor ε_{bulk} (Elsner et al., 2005). The apparent kinetic isotope effect is retrieved from ε_{bulk} by taking into account both the non-reacting carbons and intramolecular competition. Although an improvement of the data collected from CSIA is thus achieved, a generic method for direct position-specific isotope analysis (PSIA) would be a valuable complement, by giving a better picture of the process (physical, chemical, biochemical or physiological) under investigation. Thus, PSIA could help to determine if there are counteractive contributions of normal and inverse isotope effects at different positions of the studied molecule that can result in a small bulk isotope effect measured with irm-MS.

Three methods are currently available for PSIA. The oldest is the chemical and/or enzymatic degradation of the molecule, with subsequent analysis of the resulting fragments by irm-MS (Meinschein et al., 1974; Monson and Hayes, 1982; Rinaldi et al., 1974; Weilacher et al., 1996). From the $\delta^{13}C$ of the fragments, the complete isotopic distribution can be rebuilt, assuming that all steps are quantitative or that their specific associated fractionation is known. Alternatively fragmentation is done by pyrolysis, coupled on-line to irm-MS (Corso and Brenna, 1997; Dias et al., 2002; Yamada et al., 2002). While this is effective for small molecules such as lactic and acetic acids (Hattori et al., 2011), ethanol (Gilbert et al., 2012) and methyl *tert*-butylether (MTBE) (Gauchotte et al., 2009), it is not applicable to larger compounds. A similar approach has been proposed for the determination of the intramolecular composition of isoproturon by combining an injector/capillary reactor coupled to irm-GC/MS (Penning and Elsner, 2007). All these methodologies work well on specific molecules for which the fragmentation is feasible, but are not of generic application. In contrast, isotope ratio monitoring of ^{2}H or ^{13}C by NMR (irm-^{2}H NMR, irm-^{13}C NMR) spectrometry gives access directly to all spectrally-resolved sites in the compound, thus position-specific measurements.

The use of ^{2}H NMR spectrometry was developed during the early 1980s (Martin and Martin, 1981). Nowadays, PSIA by NMR for $\delta^{2}H_i$ determination is routinely used for metabolic and climatic analyses and as a tool for authentication (for reviews see (Jamin and Martin, 2006; Martin et al., 2006a, 2006b, 2006c)). The use of irm-^{13}C NMR presented more of a challenge because the range of isotopic variation in natural compounds is about 10-fold less for ^{13}C than for ^{2}H (about 50‰ and 500‰, respectively, on the δ-scale). Hence, irm-^{13}C NMR requires 10-times higher precision: a standard deviation for the long term repeatability lower than 1‰ is the normal requirement. As a result, the development of the technique took longer, starting from the first work (Caer et al., 1991) to the recent attainment of suitable acquisition conditions (Caytan et al., 2007a). A relative method of ^{13}C NMR was previously proposed as a way to calculate isotope effects in which the NMR signal intensity of the site-active carbon is related to the intensity of the signal of a 'neutral' carbon (far away from the active site), making the assumption that the latter is not modified during the chemical reaction (Singleton and Thomas, 1995). While valuable for studying individual reactions, this method, being relative, is not suitable for studies of all carbon positions, as required by PSIA. Our work, has now made it possible to express the ^{13}C-content of the isotopic composition on the δ-scale (‰) by exploiting irm-^{13}C NMR combined with the $\delta^{13}C_{bulk}$ obtained by irm-EA/MS. The completion of the method using an external calibrated reference (Caytan et al., 2007a) was ensured by solving the two main constraints: (i) obtaining homogeneous and robust ^{1}H decoupling of $^{13}C-^{1}H$ interactions by using appropriate adiabatic decoupling sequences (Tenailleau and Akoka, 2007) and (ii) reducing the experimental time by using relaxation reagents (Caytan et al., 2007b). An exhaustive list of applications of irm-^{13}C NMR is listed in SI.

To our knowledge, studies where PSIA has been applied to molecules involved in environmental pollution are rare. We are aware of only two studies on the whole molecule, both involving MTBE: one, using pyrolysis coupled to irm-GC/MS for ^{13}C (Gauchotte et al., 2009), and the other using irm-^{2}H NMR (McKelvie et al., 2009). One paper was published recently using irm-^{13}C NMR for the determination of the relative intramolecular ^{13}C distribution in *n*-alkanes (Gilbert et al., 2013). In addition, model studies on vanillin show matrix-dependent position-specific fractionation with different isotope effects induced by sorption on normal or inverse stationary phases (Botosoa et al., 2008, 2009; Höhener et al., 2012). A study has described partial intramolecular distributions after either chemical or biochemical degradation (Penning and Elsner, 2007). A recent review pointed out that PSIA was still on "the frontiers of stable isotope geoscience" (Eiler et al., 2014). The present work aims to contribute significantly towards putting irm-^{13}C NMR as an accessible tool at that frontier, and to delineate the performance of NMR for measuring intramolecular isotope composition in the framework of environmental studies. Several aspects needed to be addressed: (i) the pertinence of PSIA over the bulk measurement, (ii) how irm-^{13}C NMR can be used for PSIA, (iii) the performance of irm-^{13}C NMR in terms of accuracy and sensitivity and (iv) the constraints of irm-^{13}C NMR versus its use on real samples.

In order to illustrate each aspect we decided to study the evaporation phenomenon which is significant in the fate of volatile pollutants (Volatile Organic Compounds, VOCs). This phenomenon has been studied by irm-MS in laboratory experiments on pure chemicals and a large bulk isotope fractionation was not observed, in contrast to the isotope effects induced by (bio)degradation. For examples, significant (even small) isotope effects were found during liquid/vapor transfer of fuel oxygenated-additives like MTBE (Kuder et al., 2009), chlorinated VOCs such as trichloroethene (TCE) (Jeannottat and Hunkeler, 2012; Poulson and Drever, 1999), and aromatic hydrocarbons such as toluene (Shin and Lee, 2010). These data prove that volatilization can induce significant normal or inverse isotope effects detected from the $\Delta\delta^{13}C_{bulk}$ values (see Table S1), depending on experimental conditions and the compound under consideration. However, it is reasonable to predict that $\Delta\delta^{13}C_i$ values (difference between $\delta^{13}C_i$ of the initial and final states) may be of a greater magnitude but that such effects are being masked by counteracting normal and inverse isotope effects at different carbon positions. We have probed this phenomenon by using irm-^{13}C NMR for PSIA. To do so, we have simulated the evaporation conditions on a model molecule, ethanol, and on three small-molecular weight pollutants: MTBE, toluene and TCE. These compounds cover different chemical structures and physicochemical properties and are therefore a pertinent choice with which to test the capability of irm-^{13}C NMR. Furthermore, studies using irm-MS have already been carried out on these molecules, which gives the opportunity to compare the results obtained in the present study with those in the literature. We selected four distinct evaporation conditions involving liquid/vapor transformation adapted from literature. Passive evaporation (PE) has been studied on benzene and toluene and it allows the observation of isotope effects induced by gas-phase diffusion and liquid/vapor transformation (Shin and Lee, 2010). Forced air-flux-assisted evaporation (AFE) was selected on the basis of the work of (Huang et al., 1999), who studied TCE and dichloromethane, with the objective to limit the contribution of gas-phase diffusion to the isotope effects. The protocol designed as low pressure evaporation (LPE) was used to eliminate gas-phase diffusion, thus to detect isotope effect generated by liquid/vapor transformation with the objective of measuring the potential effect of the diffusion layer (Kuder et al.,

2009). Finally, distillation (DE) was studied as a way to transform the liquid into vapor at atmospheric pressure at boiling temperature, within an equilibrium between a continuous evaporation–condensation process (see Table 1). Bulk ^{13}C isotopic fractionation induced by distillation has already been studied on anethole, benzene and toluene (Balabane and Létolle, 1985) and data on distillation-related effects for ethanol are also published (Baudler et al., 2006; Moussa et al., 1990; Zhang et al., 2002). These four processes (PE, AFE, LPE and DE) induce unique isotope fractionation patterns in these pollutants, which can tentatively be interpreted in terms of the presence of certain chemical features in the molecule.

2. Material and methods

2.1. Chemicals

Methyl *tert*-butylether (99.8%), toluene (99.9%) and trichloroethylene (99.5%) were obtained from Sigma–Aldrich. Absolute ethanol (99.8%) was purchased from VWR Prolabo. DMSO-d_6, dioxane-d_8 and CD_3CN were obtained from Eurisotop. Tris(2,4-pentadionato)chromium(III) [$Cr(Acac)_3$] was from Merck.

2.2. Evaporation experiments

Either 20 mL or 100 mL of pure compound was subjected to the evaporation process and the remaining substrate (2–7%) was submitted to isotope analysis. Passive evaporation (PE) was carried out with 20 mL of compound in a 30 mL vial under a fume hood at constant airflow of 2.10^5 L/h at an ambient temperature of approx. 22 °C. Forced air-flux-assisted evaporation (AFE) was performed with 20 mL of compound in a 250 mL triple-neck round bottom flasks with two necks open and the third connected to an inlet blowing air at 500 L/h at ambient temperature. Evaporation at low-pressure (LPE) was done on 20 mL of compound in a 250 mL pear-shaped flask in a 30 °C water bath and using a rotary evaporator to generate a vacuum of about 10 mbar. Distillation (DE) was carried out on 100 mL of each compound using a Cadiot distillation column equipped with a Teflon turning band at the temperatures corresponding to the boiling point for each compound.

2.3. Isotope ratio monitoring ^{13}C NMR spectrometry

The sample preparation consisted in the successive addition in a 4 mL vial of the compound, the lock substance and the relaxing agent $Cr(Acac)_3$. The respective amount of each was adapted according to (i) the T_1 values (longitudinal relaxation), (ii) the reciprocal solubility with the deuteriated solvents and/or the relaxation agent and (iii) the ^{13}C NMR spectrum: no peak overlapping. The exact preparation procedures are described in SI (Table S3).

Quantitative ^{13}C NMR spectra were recorded using an AVANCE I 400 spectrometer (Bruker Biospin, Wissembourg, France), fitted with a 5 mm i. d. $^1H/^{13}C$ dual$^+$ probe, carefully tuned at the recording frequency of 100.61 MHz, or a Bruker AVANCE III connected to a 5 mm i. d. BBFO probe tuned at the recording frequency of 100.62 MHz. The temperature of the probe was set to 303 K, without tube rotation. The exact NMR acquisition conditions are detailed in SI (Table S4).

Isotope $^{13}C/^{12}C$ ratios were calculated from processed spectra as described previously (Bayle et al., 2015, 2014), further details in SI (Table S2).

2.4. ^{13}C -irm-EA/MS

Bulk ^{13}C abundance ($\delta^{13}C_{bulk}$) was determined by irm-MS using an Integra2 spectrometer (Sercon Instruments, Crewe, UK) linked to a Sercon elemental analyser (EA) fitted with an autosampler (Sercon Instruments, Crewe, UK). A precise amount of each compound was weighted into tin capsules (2 × 5 mm, Thermo Fisher scientific) using a 10^{-6} g precision balance (Ohaus Discovery DV215CD) to give approx. 0.4 mg of compound. Great care was taken to ensure that there was no leakage from the capsule. First, during the weighing of the VOC molecule introduced into the tin-capsule, the sealed capsule was left on the balance for a short delay to verify the stability of the mass. No change in mass indicated that the capsule was effectively sealed. Secondly, the percentage of carbon was checked by the operator by comparing this value with that usually obtained on the working reference. This gives a check in relation to the intensity of the signal of the CO_2 ions. Thirdly, we have worked with a short list of samples in order to keep the time between capsules preparation and measurements to a minimum. $\delta^{13}C$ (‰) values were expressed relative to the international reference (Vienna-Pee Dee Belemnite, V-PDB) using the

Table 1
Summary of physical processes governing isotope fractionation in the experiments.

Experiment temperature	State of the liquid phase	State of the air phase	Fractionation process	References
Distillation Boiling temperature	Fully mixed (boiling)	Saturated vapor; high advective vapor flux.	Vapor-liquid isotope effect at boiling temperature	Jancso and Van Hook, 1974 and many classical papers referenced therein[a]
Low pressure evaporation T = 30 °C	Stagnant. Fast advective downward speed of liquid surface	Undersaturated vapor; high advective vapor flux	Vapor-liquid isotope effect at low temperature	
Air-flux evaporation Room temperature.	Stagnant. Small advective downward speed of liquid surface.	Thin stagnant air boundary layer above liquid; fast diffusive vapor flux	Vapor-liquid effect and diffusion effect in air boundary	Schwarzenbach et al., 2003[b]
Passive evaporation Room temperature.	Stagnant. Diffusive boundary layer on liquid side may occur.	Thick stagnant air boundary film above liquid; diffusive vapor flux	a) For air-film limited evaporation: Vapor-liquid effect and diffusion effect in air boundary b) For liquid-film limited evaporation: IE = diffusive IE in liquid	Kuder et al., 2009, Craig and Gordon, 1965,[c] Bouchard et al. 2008,[d] Jeannottat and Hunkeler 2012[e]

[a] (Jancso and Van Hook, 1974).
[b] (Schwarzenbach et al., 2003).
[c] (Kuder et al., 2009) (Craig and Gordon, 1965).
[d] (Bouchard et al., 2008).
[e] (Jeannottat and Hunkeler, 2012).

relationship $\delta^{13}C_{VPDB}(‰) = \left(\frac{R_{sample}}{R_{standard}} - 1\right) \times 1000$. The instrument was calibrated for $\delta^{13}C$ using the international reference materials NBS-22 ($\delta^{13}C_{PDB} = -30.03‰$), SUCROSE-C6 ($\delta^{13}C_{PDB} = -10.80‰$), and IAEA–CH–7 PEF-1 ($\delta^{13}C_{PDB} = -32.15‰$) (IAEA, Vienna, Austria) and instrumental deviation followed via a laboratory standard of glutamic acid.

2.5. Calculation of ε_{bulk} and ε_i

The enrichment factor ε (‰) was obtained from the isotope fractionation factor α calculated according to the common Rayleigh approach. In theory, this should be used for continuous processes only. Although this is an approximation, it is pertinent, since it has been shown that only very small differences exist between the values calculated from Equation (1) and from mathematical relationships elaborated to describe the complete vaporization process (Jeannottat and Hunkeler, 2012):

$$\varepsilon = \ln\left(\frac{\delta^{13}C_{tx} + 1000}{\delta^{13}C_{t0} + 1000}\right)\left(\frac{1000}{\ln f}\right) \quad (1)$$

where $\delta^{13}C_{t0}$ and $\delta^{13}C_{tx}$ are respectively the isotopic compositions of the starting compound (initial state) and the remaining product after evaporation (final state) and f is the degree of advancement of the reaction (further comments in SI).

3. Results and discussion

3.1. Performance of irm-^{13}C NMR methodology for PSIA

For the effective use of irm-^{13}C NMR at natural abundance, the signal-to-noise ratio (SNR) is the factor which affects directly the precision, as the relative error on the peak area S is dependent on the inverse of SNR. To ensure the validity of the data obtained, instrumental repeatability was checked. For the compounds used in the present study, SNR was $\geq$1700 and a precision of the intramolecular ^{13}C distribution, described by a standard deviation of ~0.2–0.3‰ for all compounds studied and for each carbon position was obtained, as illustrated in Table 2 for ethanol used as reference. This precision, previously observed (Bayle et al., 2015, 2014; Caytan et al., 2007a; Gilbert et al., 2011), is suitable for the determination of $\Delta\delta^{13}C_i$ in the framework of studies on the fate of pollutants. It is also the standard deviation usually accepted in CSIA (Hofstetter and Berg, 2011; Kuder et al., 2009).

The question then is what is the threshold on the ε-range below which the isotope fractionation is not significant? This issue has been addressed by several authors, either in reviews or during the interpretation of their results (Elsner et al., 2012; Hofstetter and Berg, 2011; Jeannottat and Hunkeler, 2012; Sherwood Lollar et al., 2007; Thullner et al., 2012). Slater was among the first to point out that a $\Delta\delta^{13}C$ value lower than ~1‰ (with the standard deviation of that time, 2003) should lead to non-significant enrichment factors (Slater, 2003). It is straightforward to calculate the expanded uncertainty U associated with the $\Delta\delta^{13}C_i$ measurement by irm-^{13}C NMR. Taking plus or minus the variation range at the 95% confidence level, this is evaluated as ~0.8–0.9‰, using a standard deviation of 0.2–0.3‰ and a double measurement: analyte in the initial and final states. This value was calculated from the uncertainty estimation described by the 'guide of expression of uncertainty in measurement' GUM (JCGM/WG, 2008). For convenience, this upper limit could be expressed on the ε-scale by applying the same approach on the measurand of Equation (1) (see experimental section). For the first test during the DE process on ethanol (Table 1), as an example, a value of 0.2‰ (rounded value, using a factor $k = 2$, $\alpha = 0.05$) is obtained for the expanded uncertainty of ε_i (further details in SI). This value is slightly overestimated but covers all sources of variability, including the process used for evaporation.

This is therefore the threshold of the significance of each ε_i, i.e. below this value there is no significant fractionation for the site i (broken line on the graphics of Fig. 1). It is of the same magnitude as data found in the literature (Jeannottat and Hunkeler, 2012). Hence, the accuracy of $\Delta\delta^{13}C$ is the same for both techniques, irm-^{13}C NMR and irm-^{13}C GC/MS. To be complete, it should be mentioned that a slight dependence of the NMR response, and therefore of $\delta^{13}C_i$, with the molecule studied and the NMR spectrometer used has been shown by ring testing (Chaintreau et al., 2013). This can be normalized by applying a suitable correction factor. However, in the present case all measurements used the same NMR spectrometer, so the direct comparison $\Delta\delta^{13}C = \delta^{13}C_{final} - \delta^{13}C_{initial}$ is valid without correction.

3.2. Bulk ^{13}C fractionation during evaporation processes obtained by irm-MS

We have shown above that each evaporation process is robust since a very similar trend is observed for the isotope pattern

Table 2
^{13}C composition (‰) obtained by irm-EA/MS ($\delta^{13}C_{bulk}$) and by irm-^{13}C NMR ($\delta^{13}C_{CH2}$ and $\delta^{13}C_{CH3}$) of ethanol upon repetition of different volatilization processes. Each line in the Table represents one experiment.

Volatilization simulation process	Residue (%)[a]	$\delta^{13}C_{bulk}$ (‰)	$\delta^{13}C_{CH2}$ (‰)	$\delta^{13}C_{CH3}$ (‰)	ε_{bulk}
Reference	100	−27.8	−25.5	−30.1	na
			−25.6	−30.0	na
			−25.8	−29.8	na
PE[b]	7.1 (1)	−16.7	−18.8	−14.5	−6.0
	6.8 (2)	−16.4	−18.9	−13.8	−6.1
	7.2 (3)	−17.6	−19.6	−15.6	−5.6
AFE	7.3	−21.4	−21.1	−21.6	−3.3
	6.4	−21.1	−21.2	−21.1	−3.3
	5.6	−20.6	−20.9	−20.3	−3.4
LPE	4.6	−28.8	−27.8	−29.9	−0.0
	3.7	−29.1	−28.2	−30.0	+0.0
	6.0	−28.8	−27.6	−30.0	−0.0
DE	3.9	−30.0	−28.7	−31.3	+0.4
	6.9	−29.6	−28.5	−30.7	+0.3
	3.5	−29.9	−29.3	−30.7	+0.2

PE: Passive evaporation; AFE: Air flux evaporation; LPE: Low pressure evaporation; DE: distillation evaporation.
[a] Mass percentage of the remaining ethanol.
[b] Passive evaporation of samples 1 and 2 were performed during 14 days at 20–22 °C and for sample 3, it was 12 days at 26–28 °C.

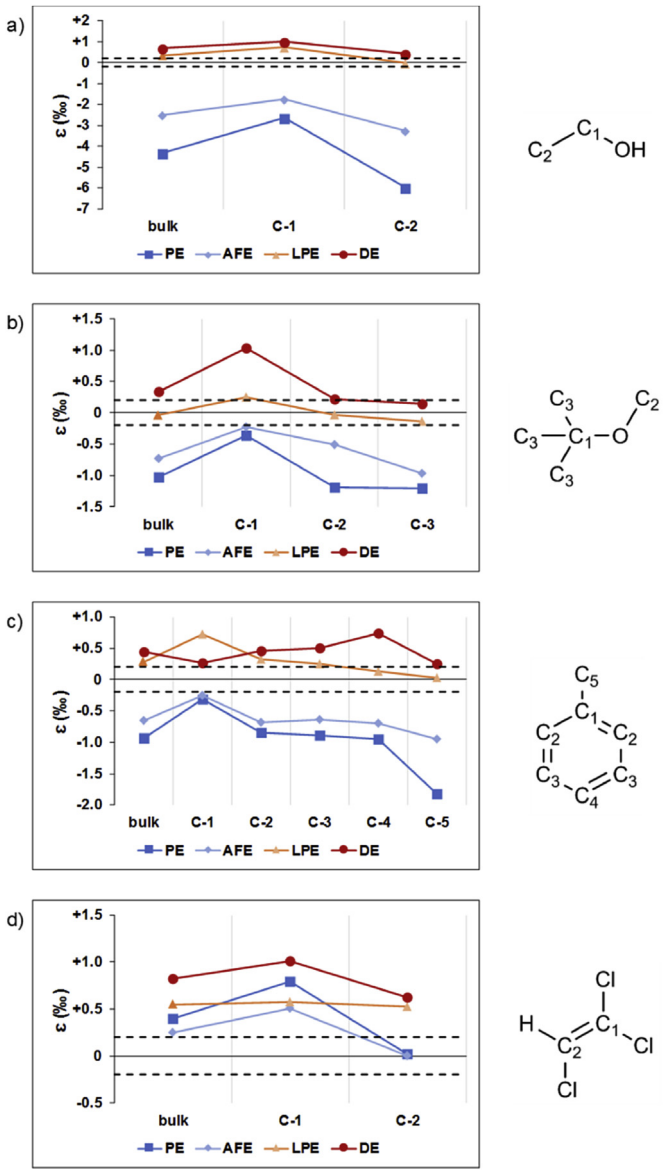

Fig. 1. Enrichment factor (‰) obtained from irm-EA/MS (bulk, ε_{bulk}) or from irm-^{13}C NMR (position-specific, ε_i) upon evaporation processes as described in the experimental section (PE = passive evaporation; AFE = air-flux evaporation; LPE = low pressure evaporation and DE = distillation). Broken black lines represent limits for significant effects. Positive enrichment factors mean an inverse isotope effect in which heavy isotopomers (^{13}C) are preferentially transferred to the gas phase: the remaining liquid is thus depleted in ^{13}C. Conversely, it is the opposite for negative enrichment factors. Also shown are the molecular structures of each compound with the carbon atoms numbered in relation to decreasing ^{13}C chemical shift in the ^{13}C NMR spectrum.

(Table 2). When we compare the irm-MS results shown in Fig. 1 with those described in previous studies the enrichment factors (ε_{bulk}) obtained compare closely when a similar process was applied on a given molecule.

Thus, the ε_{bulk} obtained in passive evaporation (PE) of MTBE of −1.0‰ (Fig. 1b) is the same as that obtained in diffusive volatilization from aqueous solution (Kuder et al., 2009). Although, the evaporation conditions are not strictly the same, volatilization of the pure solvent or from aqueous solution appears to induce the same bulk isotopic fractionation. For toluene, a $\varepsilon_{bulk} = -0.41$‰ was calculated for PE (Shin and Lee, 2010). This effect is lower than that observed during toluene evaporation in crude oil: $\varepsilon_{bulk} = -1.5$‰ (Xiao et al., 2012). The ε_{bulk} for PE of toluene found in the present work (Fig. 1c) is between these two values. Similarly, for the distillation (DE) of toluene (Fig. 1c), we obtained a small inverse effect with $\varepsilon_{bulk} = 0.4$‰, thus confirming previous results using the same device as in the present work (Balabane and Létolle, 1985). Bulk isotopic fractionation occurring during volatilization of TCE has also been studied previously. The small inverse effect obtained during PE of $\varepsilon_{bulk} = +0.4$‰ (Fig. 1d) is in good agreement with published values $\varepsilon_{bulk} = +0.3$‰ (Jeannottat and Hunkeler, 2012) and $\varepsilon_{bulk} = +0.4$‰ (Poulson and Drever, 1999). During an air-flux assisted evaporation (AFE) experiment a $\varepsilon_{bulk} = 0.3$‰ was found (Huang et al., 1999), very close to the value found in this study, $\varepsilon_{bulk} = 0.2$‰ (Fig. 1d).

To sum up, bulk normal isotope effects are observed during evaporation (PE and AFE experiments), contrasting with the bulk inverse effects found under distillation (DE). The only exception to these general trends is for TCE for which inverse isotope effects were measured for all volatilization modes.

3.3. Intramolecular ^{13}C fractionation upon evaporation obtained by irm-^{13}C NMR

3.3.1. Ethanol

The criteria for the accuracy of irm-^{13}C NMR having been established, the repeatability of molecular behavior in relation to the evaporation processes could be addressed. Initially, three replicates of each volatilization simulation were performed with ethanol as model compound. The environmental conditions (in particular, temperature and pressure of the laboratory) were not imposed and could differ slightly between replicates. Therefore the calculation of a mean value of $\Delta\delta^{13}$C is inappropriate. However, the ε_i values obtained indicate a close repeatability when the 3 experiments of a given process have been performed simultaneously. For PE, the temperature and duration were modified for the third experiment: 14 days at 20–22 °C for the two first experiments and 12 days at 26–28 °C for the third (Table 2). Nevertheless, this change in experimental conditions only slightly affected the results for PSIA. The ε_i values of one experiment for each process are displayed in Fig. 1a. The intramolecular data from the distillation experiment are in agreement with previous studies (Botosoa et al., 2008; Caytan et al., 2007a).

3.3.2. MTBE

Results obtained during liquid/vapor transformation of MTBE are depicted in Fig. 1b. The methyl groups (C-3 and C-2) show significant normal isotope effects during PE, dictating the observed ε_{bulk}. In contrast, when evaporation is forced by low pressure (LPE) or elevated temperature (DE) the C-1 position is dominant and displays an inverse isotope effect, noticeably during distillation (DE). In each case it is notable how each position shows an individual behavior, indicating how the overall effect ε_{bulk} observed under altered evaporation conditions can have the same value but for different reasons. An interesting outcome of these experiments is that when MTBE undergoes PE or AFE in the environment this will induce a change in its ^{13}C/^{12}C ratio at the C-2 and C-3, whereas C-1 will remain essentially unaltered. Volatilization is of course, only one cause of ^{13}C isotopic fractionation in the environment: other phenomena such as sorption or (bio)degradation also play a role. Nevertheless, these results clearly demonstrate that isotopic ^{13}C NMR is a good complementary tool to provide information about MTBE cycles in the environment or in forensic discrimination.

3.3.3. Toluene

The bulk isotope effect is weak, whatever the evaporation process involved and the position-specific fractionation profiles are in

the same overall sense as those for ethanol and MTBE but are of lower amplitude (Fig. 1c). It is noteworthy that, for PE and AFE it is the C-5 methyl of toluene—the lateral chain position—that is most susceptible to normal fractionation. In contrast, the most 'encumbered' position—the C-1 of toluene —is the least fractionated. The same profile is observed for LPE and DE, with inverse fractionation. In these circumstances, however, it is the ring carbons of toluene that fractionate the most. These observations merit further investigation.

3.3.4. Trichloroethene

TCE represents a distinctly different molecular structure, dominated by the three chlorine atoms. As previously found in the literature (Jeannottat and Hunkeler, 2012; Poulson and Drever, 1999) the behavior of TCE from each volatilization mode is markedly different from the other compounds studied (Fig. 1d). Under all evaporation conditions both the bulk and the position-specific fractionation for both carbon atoms is inverse. Furthermore, under the evaporation modes PE and AFE, to which gas-phase diffusion contributes, all the fractionation can be assigned to the position carrying 2 atoms of chlorine. In contrast, for evaporation forced with low-pressure or high temperature (LPE, DE) $^{13}C_i$ isotopic fractionation is observed at both positions.

3.3.5. Governing physical processes

The resulting isotope effects in the four evaporation modes are a combination of equilibrium vapor pressure, kinetic and diffusive isotope effects, and must therefore be discussed with respect to the physical processes active in each evaporation mode. This discussion is summarized in Table 1. The most important difference between the first two modes (DE and LPE) and the latter two (AFE and PE) is the existence of a diffusion limitation at the liquid-air boundary. As discussed by Kuder et al., one of two diffusive films – either the liquid boundary layer or the air-film boundary layer – may create a diffusive isotope effect (Kuder et al., 2009). This isotope effect is known always to be normal and may shift enrichment factors from inverse to normal. This is the case here for ethanol, MTBE and toluene.

Only TCE does not follow this trend, suggesting that the diffusion effect is smaller than the inverse equilibrium vapor pressure effect (Jeannottat and Hunkeler, 2012). A more quantitative interpretation of such physical effects is presently difficult due to the low number of compounds studied by irm-^{13}C NMR, but will be presented in a future work in which isotope fractionation for more compounds will be assessed.

Two further phenomena anticipated on the basis of prior studies (Botosoa et al., 2008, 2009) are also confirmed. First, for some cases where ε_{bulk} is non-significant (<0.2‰), we observe ε_i with significant positive or negative values, as shown, for MTBE (DE, Fig. 1b), for toluene (LPE and DE, Fig. 1c) and for TCE (AFE, Fig. 1d). Secondly, for some values of ε_{bulk} that are very similar, the positional isotope fractionation differs significantly, for example: toluene (LPE and DE, Fig. 1c) and TCE (PE and AFE, Fig. 1d) (note that ε_{bulk} is the mean contribution of all ε_i). It can be anticipated that the vapor–liquid isotope effect might be fairly specific for distinct positions of carbon in the molecule, especially in liquids with hydrogen bonding. Such effects have been demonstrated for $^2H/^1H$ fractionation (Zhang et al., 2002). In contrast, the isotope effect for diffusion in the gas phase should, *a priori*, not be site-specific.

4. Conclusion

The data presented in this study fully support our working hypothesis: by exploiting PSIA it is possible to assess progressive evaporation even for compounds where the bulk isotope effect is small. This approach should help to obtain new insights into the molecular parameters involved in evaporation processes.

At present, those interactions which are responsible for this differential fractionation remain to be better quantified. Work is in progress to apply PSIA to a larger number of organic liquids in order to propose a model giving a better prediction of the expression of the two competing isotope effects: vapor–liquid and diffusion. This will give new clues on the quantification of the evaporation which plays an important role in physical remediation.

It is clear that irm-NMR offers enormous potential to the field of environment science, notably as a complement to CSIA for the refinement of existing models. Although the performance of irm-^{13}C NMR is equivalent to irm-GC/MS, constraints might appear when working with dilute samples. It should be noted that although NMR suffers from lower sensitivity compared with irm-GC/MS, this is not due to a limit of quantification (LOQ). In contrast to other techniques, the NMR signal can be accumulated until the desired signal-to-noise ratio is attained. So, in theory only a few milligrams of sample can be used. The problem would be just sensitivity. To be able to run analyses in acceptable time, with several milligrams only, the duration of the irm-^{13}C NMR spectral acquisition will be of several days, thus far from any interest for routine application. Nonetheless, there is reasonable potential for real cases to be studied by irm-^{13}C NMR used as a forensic tool by comparing a direct site early sampling at the very early course of the pollution and a sample from a potential source (see an example in SI). But, as a first application of irm-^{13}C NMR, it is the refinement of existing models that is of primary interest. Therefore, even though only pure chemicals are used in the present study, the information obtained gives new insight into the intrinsic isotope profile related to a given evaporation mode. The same approach could be extended to other type of transformation (biotic or abiotic). Improvements in sensitivity recently proposed include using modified NMR pulse sequences, exploiting polarization transfer (Thibaudeau et al., 2010) and 2D NMR (Martineau et al., 2013). Such developments, associated with the continuous improvement of sensitivity of the NMR spectrometer should bring down the amount of material required by 10–15 fold in the near future, i.e. to around 25 mg, rather than the 300–400 mg used in the present study, while retaining an acceptable duration for the analysis. Nonetheless, this is still a much higher mass than that needed in irm-GC/MS (about 12 ng of carbon) and the technique is likely to remain restricted to field applications involving substantial spills for the foreseeable future. In these instances, this method should be able to provide new insight to improve our understanding of isotope fractionation during remediation.

Acknowledgment

This work is funded by the French National Research Agency ANR, project ISOTO-POL funded by the program CESA (N° 009 01). M. Julien thanks the ANR for funding his PhD bursary through this project. K. Bayle thanks the financial support from the French Research Ministry.

Appendix A. Supplementary data

Supplementary data related to this article can be found at http://dx.doi.org/10.1016/j.envpol.2015.05.047.

References

Aelion, C.M., Höhener, P., Hunkeler, D., Aravena, R., 2010. Environmental Isotopes in Biodegradation and Bioremediation. CRC; Taylor & Francis [distributor], Boca Raton, Fla; London.

Balabane, M., Létolle, R., 1985. Inverse overall isotope fractionation effect through distillation of some aromatic molecules (anethole, benzene and toluene). Chem. Geol. Isot. Geosci. Sect. 52, 391–396.
Baudler, R., Adam, L., Rossmann, A., Versini, G., Engel, K.-H., 2006. Influence of the distillation step on the ratios of stable isotopes of ethanol in cherry brandies. J. Agric. Food Chem. 54, 864–869.
Bayle, K., Akoka, S., Remaud, G.S., Robins, R.J., 2015. Nonstatistical ^{13}C distribution during carbon transfer from glucose to ethanol during fermentation is determined by the catabolic pathway exploited. J. Biological Chem. 290, 4118–4128.
Bayle, K., Gilbert, A., Julien, M., Yamada, K., Silvestre, V., Robins, R.J., Akoka, S., Yoshida, N., Remaud, G.S., 2014. Conditions to obtain precise and true measurements of the intramolecular ^{13}C distribution in organic molecules by isotopic ^{13}C nuclear magnetic resonance spectrometry. Anal. Chim. Acta 846, 1–7.
Botosoa, E.P., Caytan, E., Silvestre, V., Robins, R.J., Akoka, S., Remaud, G.S., 2008. Unexpected fractionation in site-specific ^{13}C isotopic distribution detected by quantitative ^{13}C NMR at natural abundance. J. Am. Chem. Soc. 130, 414–415.
Botosoa, E.P., Silvestre, V., Robins, R.J., Rojas, J.M.M., Guillou, C., Remaud, G.S., 2009. Evidence of ^{13}C non-covalent isotope effects obtained by quantitative ^{13}C nuclear magnetic resonance spectroscopy at natural abundance during normal phase liquid chromatography. J. Chromatogr. A 1216, 7043–7048.
Böttcher, M.E., Schnetger, B., 2004. Chapter 27-Direct measurement of the content and isotopic composition of sulfur in black shales by means of combustion-isotope-ratio-monitoring mass spectrometry (C-irmMS). In: Groot, P.A.d. (Ed.), Handbook of Stable Isotope Analytical Techniques. Elsevier, Amsterdam, pp. 597–603.
Bouchard, D., Höhener, P., Hunkeler, D., 2008. Carbon isotope fractionation during volatilization of petroleum hydrocarbons and diffusion across a porous medium: a column Experiment. Environ. Sci. Technol. 42, 7801–7806.
Brand, W.A., 1996. High precision isotope ratio monitoring techniques in mass spectrometry. J. Mass Spectrom. 31, 225–235.
Caer, V., Trierweiler, M., Martin, G.J., Martin, M.L., 1991. Determination of site-specific carbon isotope ratios at natural abundance by carbon-13 nuclear magnetic resonance spectroscopy. Anal. Chem. 63, 2306–2313.
Caytan, E., Botosoa, E.P., Silvestre, V., Robins, R.J., Akoka, S., Remaud, G.S., 2007a. Accurate quantitative ^{13}C NMR Spectroscopy: repeatability over time of site-specific ^{13}C isotope ratio determination. Anal. Chem. 79, 8266–8269.
Caytan, E., Remaud, G.S., Tenailleau, E., Akoka, S., 2007b. Precise and accurate quantitative ^{13}C NMR with reduced experimental time. Talanta 71, 1016–1021.
Chaintreau, A., Fieber, W., Sommer, H., Gilbert, A., Yamada, K., Yoshida, N., Pagelot, A., Moskau, D., Moreno, A., Schleucher, J., Reniero, F., Holland, M., Guillou, C., Silvestre, V., Akoka, S., Remaud, G.S., 2013. Site-specific ^{13}C content by quantitative isotopic ^{13}C nuclear magnetic resonance spectrometry: a pilot inter-laboratory study. Anal. Chim. Acta 788, 108–113.
Cincinelli, A., Pieri, F., Zhang, Y., Seed, M., Jones, K.C., 2012. Compound specific isotope analysis (CSIA) for chlorine and bromine: a review of techniques and applications to elucidate environmental sources and processes. Environ. Pollut. 169, 112–127.
Corso, T.N., Brenna, J.T., 1997. High-precision position-specific isotope analysis. Proc. Natl. Acad. Sci. 94, 1049–1053.
Craig, H., Gordon, L.I., 1965. In: Tongiorgi, E. (Ed.), Conference on Stable Isotopes in Oceanographic Studies and Paleotemperatures. Italy, 9–130.
Crosson, E.R., Ricci, K.N., Richman, B.A., Chilese, F.C., Owano, T.G., Provencal, R.A., Todd, M.W., Glasser, J., Kachanov, A.A., Paldus, B.A., Spence, T.G., Zare, R.N., 2002. Stable isotope ratios using cavity ring-down Spectroscopy: determination of $^{13}C/^{12}C$ for carbon dioxide in human breath. Anal. Chem. 74, 2003–2007.
Dias, R.F., Freeman, K.H., Franks, S.G., 2002. Gas chromatography–pyrolysis–isotope ratio mass spectrometry: a new method for investigating intramolecular isotopic variation in low molecular weight organic acids. Org. Geochem. 33, 161–168.
Eiler, J.M., Bergquist, B., Bourg, I., Cartigny, P., Farquhar, J., Gagnon, A., Guo, W., Halevy, I., Hofmann, A., Larson, T.E., Levin, N., Schauble, E.A., Stolper, D., 2014. Frontiers of stable isotope geoscience. Chem. Geol. 372, 119–143.
Ellis, L., Fincannon, A.L., 1998. Analytical improvements in irm-GC/MS analyses: advanced techniques in tube furnace design and sample preparation. Org. Geochem. 29, 1101–1117.
Elsner, M., Jochmann, M.A., Hofstetter, T.B., Hunkeler, D., Bernstein, A., Schmidt, T.C., Schimmelmann, A., 2012. Current challenges in compound-specific stable isotope analysis of environmental organic contaminants. Anal. Bioanal. Chem. 403, 2471–2491.
Elsner, M., Zwank, L., Hunkeler, D., Schwarzenbach, R.P., 2005. A new concept linking observable stable isotope fractionation to transformation pathways of organic pollutants. Environ. Sci. Technol. 39, 6896–6916.
Galimov, E.M., 2006. Isotope organic geochemistry. Org. Geochem. 37, 1200–1262.
Gauchotte, C., O'Sullivan, G., Davis, S., Kalin, R.M., 2009. Development of an advanced on-line position-specific stable carbon isotope system and application to methyl *tert*-butyl ether. Rapid Commun. Mass Spectrom. 23, 3183–3193.
Gilbert, A., Hattori, R., Silvestre, V., Wasano, N., Akoka, S., Hirano, S., Yamada, K., Yoshida, N., Remaud, G.S., 2012. Comparison of IRMS and NMR spectrometry for the determination of intramolecular ^{13}C isotope composition: application to ethanol. Talanta 99, 1035–1039.
Gilbert, A., Silvestre, V., Segebarth, N., Tcherkez, G., Guillou, C., Robins, R.J., Akoka, S., Remaud, G.S., 2011. The intramolecular ^{13}C-distribution in ethanol reveals the influence of the CO_2-fixation pathway and environmental conditions on the site-specific ^{13}C variation in glucose. Plant Cell Environ. 34, 1104–1112.
Gilbert, A., Yamada, K., Yoshida, N., 2013. Exploration of intramolecular ^{13}C isotope distribution in long chain n-alkanes (C11–C31) using isotopic ^{13}C NMR. Org. Geochem. 62, 56–61.
Hattori, R., Yamada, K., Kikuchi, M., Hirano, S., Yoshida, N., 2011. Intramolecular carbon isotope distribution of acetic acid in vinegar. J. Agric. Food Chem. 59, 9049–9053.
Hofstetter, T.B., Berg, M., 2011. Assessing transformation processes of organic contaminants by compound-specific stable isotope analysis. TrAC Trends Anal. Chem. 30, 618–627.
Höhener, P., Silvestre, V., Lefrançois, A., Loquet, D., Botosoa, E.P., Robins, R.J., Remaud, G.S., 2012. Analytical model for site-specific isotope fractionation in ^{13}C during sorption: determination by isotopic ^{13}C NMR spectrometry with vanillin as model compound. Chemosphere 87, 445–452.
Huang, L., Sturchio, N.C., Abrajano Jr., T., Heraty, L.J., Holt, B.D., 1999. Carbon and chlorine isotope fractionation of chlorinated aliphatic hydrocarbons by evaporation. Org. Geochem. 30, 777–785.
Jamin, E., Martin, G., 2006. SNIF-NMR – Part 4: applications in an economic context: the example of wines, spirits, and juices. In: Webb, G. (Ed.), Modern Magnetic Resonance. Springer, Netherlands, pp. 1681–1687.
Jancso, G., Van Hook, W.A., 1974. Condensed phase isotope effects. Chem. Rev. 74, 689–750.
JCGM/WG, 2008. Evaluation of Measurement Data- Guide to the Expression of Uncertainty in Measurement, vol. 100.
Jeannottat, S., Hunkeler, D., 2012. Chlorine and carbon isotopes fractionation during volatilization and diffusive transport of trichloroethene in the unsaturated zone. Environ. Sci. Technol. 46, 3169–3176.
Kuder, T., Philp, P., Allen, J., 2009. Effects of volatilization on carbon and hydrogen isotope ratios of MTBE. Environ. Sci. Technol. 43, 1763–1768.
Malinovsky, D., Dunn, P.J.H., Goenaga-Infante, H., 2013. Determination of absolute $^{13}C/^{12}C$ isotope amount ratios by MC-ICPMS using calibration with synthetic isotope mixtures. J. Anal. Atomic Spectrom. 28, 1760–1771.
Martin, G., Martin, M., Remaud, G., 2006a. SNIF-NMR – part 3: from mechanistic affiliation to origin inference. In: Webb, G. (Ed.), Modern Magnetic Resonance. Springer, Netherlands, pp. 1669–1680.
Martin, G.J., Akoka, S., Martin, M.L., 2006b. SNIF-NMR – part 1: principles. In: Webb, G.A. (Ed.), Modern Magnetic Resonance. Springer, Berlin, pp. 1651–1658.
Martin, G.J., Martin, M.L., 1981. Deuterium labelling at the natural abundance level as studied by high field quantitative ^{2}H NMR. Tetrahedron Lett. 22, 3525–3528.
Martin, M., Zhang, B., Martin, G., 2006c. SNIF-NMR – part 2: isotope ratios as tracers of chemical and biochemical mechanistic pathways. In: Webb, G. (Ed.), Modern Magnetic Resonance. Springer, Netherlands, pp. 1659–1667.
Martineau, E., Akoka, S., Boisseau, R., Delanoue, B., Giraudeau, P., 2013. Fast quantitative $^{1}H–^{13}C$ two-dimensional NMR with very high precision. Anal. Chem. 85, 4777–4783.
Matthews, D.E., Hayes, J.M., 1978. Isotope-ratio-monitoring gas chromatography-mass spectrometry. Anal. Chem. 50, 1465–1473.
McKelvie, J.R., Hyman, M.R., Elsner, M., Smith, C., Aslett, D.M., Lacrampe-Couloume, G., Sherwood Lollar, B., 2009. Isotopic fractionation of methyl tert-butyl ether suggests different initial reaction mechanisms during aerobic biodegradation. Environ. Sci. Technol. 43, 2793–2799.
Meinschein, W.G., Rinaldi, G.G.L., Hayes, J.M., Schoeller, D.A., 1974. Intramolecular isotopic order in biologically produced acetic acid. Biol. Mass Spectrom. 1, 172–174.
Monson, K.D., Hayes, J.M., 1982. Carbon isotopic fractionation in the biosynthesis of bacterial fatty acids. Ozonolysis of unsaturated fatty acids as a means of determining the intramolecular distribution of carbon isotopes. Geochim. Cosmochim. Acta 46, 139–149.
Moussa, I., Naulet, N., Martin, M.L., Martin, G.J., 1990. A site-specific and multielement approach to the determination of liquid-vapor isotope fractionation parameters: the case of alcohols. J. Phys. Chem. 94, 8303–8309.
Muccio, Z., Jackson, G.P., 2009. Isotope ratio mass spectrometry. Analyst 134, 213–222.
Penning, H., Elsner, M., 2007. Intramolecular carbon and nitrogen isotope analysis by quantitative dry fragmentation of the phenylurea herbicide isoproturon in a combined injector/capillary reactor prior to GC separation. Anal. Chem. 79, 8399–8405.
Poulson, S.R., Drever, J.I., 1999. Stable isotope (C, Cl, and H) fractionation during vaporization of trichloroethylene. Environ. Sci. Technol. 33, 3689–3694.
Rinaldi, G., Meinschein, W.G., Hayes, J.M., 1974. Intramolecular carbon isotopic distribution in biologically produced acetoin. Biol. Mass Spectrom. 1, 415–417.
Sano, M., Yotsui, Y., Abe, H., Sasaki, S., 1976. A new technique for the detection of metabolites labelled by the isotope ^{13}C using mass fragmentography. Biol. Mass Spectrom. 3, 1–3.
Santamaria-Fernandez, R., Carter, D., Hearn, R., 2008. Precise and traceable $^{13}C/^{12}C$ isotope amount ratios by multicollector ICPMS. Anal. Chem. 80, 5963–5969.
Schwarzenbach, R.P., Gschwend, P.M., Imboden, D.M., 2003. Environmental Organic Chemistry, second ed. Wiley, Hoboken, New Jersey.
Sherwood Lollar, B., Hirschorn, S.K., Chartrand, M.M.G., Lacrampe-Couloume, G., 2007. An approach for assessing total instrumental uncertainty in compound-specific carbon isotope Analysis: implications for environmental remediation studies. Anal. Chem. 79, 3469–3475.
Shin, W.J., Lee, K.S., 2010. Carbon isotope fractionation of benzene and toluene by progressive evaporation. Rapid Commun. Mass Spectrom. 24, 1636–1640.
Singleton, D.A., Thomas, A.A., 1995. High-precision simultaneous determination of multiple small kinetic isotope effects at natural abundance. J. Am. Chem. Soc. 117, 9357–9358.

Slater, G.F., 2003. Stable isotope forensics–when isotopes work. Environ. Forensics 4, 13–23.
Smallwood, B.J., Paul Philp, R., Allen, J.D., 2002. Stable carbon isotopic composition of gasolines determined by isotope ratio monitoring gas chromatography mass spectrometry. Org. Geochem. 33, 149–159.
Tenailleau, E., Akoka, S., 2007. Adiabatic ^{1}H decoupling scheme for very accurate intensity measurements in ^{13}C NMR. J. Magn. Reson. 185, 50–58.
Thibaudeau, C., Remaud, G.r., Silvestre, V., Akoka, S., 2010. Performance evaluation of quantitative adiabatic ^{13}C NMR pulse sequences for site-specific isotopic measurements. Anal. Chem. 82, 5582–5590.
Thullner, M., Centler, F., Richnow, H.-H., Fischer, A., 2012. Quantification of organic pollutant degradation in contaminated aquifers using compound specific stable isotope analysis – review of recent developments. Org. Geochem. 42, 1440–1460.
Weilacher, T., Gleixner, G., Schmidt, H.-L., 1996. Carbon isotope pattern in purine alkaloids a key to isotope discriminations in C1 compounds. Phytochemistry 41, 1073–1077.
Xiao, Q., Sun, Y., Zhang, Y., Chai, P., 2012. Stable carbon isotope fractionation of individual light hydrocarbons in the C6–C8 range in crude oil as induced by natural evaporation: experimental results and geological implications. Org. Geochem. 50, 44–56.
Yamada, K., Tanaka, M., Nakagawa, F., Yoshida, N., 2002. On-line measurement of intramolecular carbon isotope distribution of acetic acid by continuous-flow isotope ratio mass spectrometry. Rapid Commun. Mass Spectrom. 16, 1059–1064.
Zhang, B.-L., Jouitteau, C., Pionnier, S., Gentil, E., 2002. Determination of multiple equilibrium isotopic fractionation factors at natural abundance in liquid-vapor transitions of organic molecules. J. Phys. Chem. B 106, 2983–2988.